Research Article/Araştırma Makalesi

gazi JOURNAL OF ENGINEERING SCIENCES

Gazi AKADEMİK YAYINCILIK

GAZİ
JOURNAL OF ENGINEERING SCIENCES

The Effects of Infill Geometry and Porosity Ratio on Mechanical Properties of PLA Structures Produced by Additive Manufacturing

Rukiye Yeşiloğlu[a], Ramazan Özmen[b*], Mustafa Günay[c]

Submitted: 24.01.2023 Revised: 29.05.2023 Accepted: 08.07.2023 doi:10.30855/gmbd.0705071

ABSTRACT

The fabrication of intricately formed parts, challenging with the traditional manufacturing approach, is facilitated by additive manufacturing (AM). Stacking the material layer by layer and using the 3D data from the model, parts are created using this technique. The design of parts with various porosities inside the same cell structure and industry sector-specific manufacture are both made possible by this technology. With varied infill geometries and porosity ratios, pieces made from PLA material with different mechanical properties were compared in this study. Parts were made for this purpose using fused deposition modeling (FDM) and various infill geometries (Octet, Gyroid, and Cross). The unit cell size for infill geometries was set at 5x5x5mm, and test samples with porosities of 50%, 30%, and 20% were created. Tensile, compression, and impact tests were conducted to examine the mechanical behavior of these parts, and the best unit cell structure was selected based on the assessed mechanical properties. In general, it was found that all fill geometries' mechanical qualities declined with increasing porosity ratio. The Octet infill geometry structure had the maximum tensile strength. However, the Cross infill geometry sample had the most significant deformation.

Keywords: Additive manufacturing, fused deposition, infill geometry, mechanical property, plastic material

[a] Karabuk University,
Institute of Graduate Programs
78050 - Karabük, Türkiye

[b*] Karabuk University,
Faculty of Engineering,
Dept. of Mechatronics Engineering
78050 - Karabük, Türkiye
Orcid: 0000-0002-6020-8538
e mail:ramazanozmen@karabuk.edu.tr

[c] Karabuk University,
Faculty of Engineering,
Dept. of Mechanical Engineering
78050 - Karabük, Türkiye
Orcid: 0000-0002-1281-1359
e mail:megunay@karabuk.edu.tr

*Corresponding author:
ramazanozmen @karabuk.edu.tr

Eklemeli İmalat ile Üretilen PLA Yapılarda Dolgu Geometrisi ve Gözenek Oranının Mekanik Özelliklere Etkisi

ÖZ

Eklemeli imalat (Eİ) yöntemi, geleneksel üretim teknikleri ile imalatı zor olan kompleks geometrili parçaların kolay bir şekilde üretilmesini sağlayan bir imalat metodudur. Bu imalat yönteminde, üretilecek olan modelin 3D verileri yardımıyla malzeme katmanlar halinde yığılarak parçalar üretilmektedir. Eriyik yığma modelleme (EYM) yöntemi termoplastik malzemelerden parça üretiminde sıklıkla kullanılan bir Eİ yöntemidir. Bu çalışmada, PLA malzemeden üretilen parçalarda farklı dolgu geometrisi ve gözenek oranının bu parçaların mekanik özelliklerine etkisi deneysel olarak incelenmiştir. Parçaların mekanik davranışlarını araştırmak amacıyla çekme, basma ve darbe deneyleri ilgili standartlara göre yapılmış ve karşılaştırılan mekanik özellikler açısından en uygun birim hücre yapısı belirlenmiştir. Bu amaçla, farklı dolgu geometrilerine (Octet, Gyroid ve Cross) ve gözenek oranlarına (%50, %30 ve %20) sahip numuneler birim hücre boyutu 5x5x5mm olacak şekilde her bir deney standardına uygun boyutlarda modellenmiş ve EYM yöntemiyle üretilmiştir. Genel olarak, tüm dolgu geometrilerinde gözeneklilik oranının artmasıyla mekanik özelliklerin kötüleştiği görülmüştür. Octet dolgu geometrili yapıda en yüksek çekme dayanımı elde edilirken, Cross dolgu geometrili yapıda en fazla şekil değişimi görülmüştür.

Anahtar Kelimeler: Eklemeli İmalat, eriyik yığma, dolgu geometrisi, mekanik özellik, plastik malzeme

To cite this article: R. Yeşiloğlu, R. Özmen and M. Gunay, "The Effects of Infill Geometry and Porosity Ratio on Mechanical Properties of PLA Structures Produced by Additive Manufacturing," *Gazi Journal of Engineering Sciences,* vol. 9, no. 2, pp. 291-303, 2023. doi:10.30855/gmbd.0705071

1. Introduction

Depending on the development of technology, the demand for special products is increasing with improved geometry, weight/strength, and aesthetics that can be used in different areas. Traditional machining methods may be insufficient to meet the geometrically optimized part/product needs and increase product demands, especially to provide the desired strength. For this purpose, different production technologies are being developed apart from traditional production methods. In contrast to machining, manufacturing technologies (plastic forming, additive manufacturing, welding, casting, etc.) in which materials are shaped by adding a wide range of product needs can be met. In this context, additive manufacturing methods, also known as three-dimensional (3D) manufacturing, which entered our lives with the developing technology, have begun to be used in all industries. In this production method, a piece that is difficult to produce with the machining method can be designed in 3D in a computer environment and produced in layers. In this manufacturing technology, parts with complex geometries can be produced at affordable costs, and industrial parts from many different materials such as plastic, ceramic, metal, or composite.

The additive manufacturing (AM) method allows structures to be built relatively quickly with highly complex infill geometries. With technological advances, the AM, which has been used for producing non-functional prototypes for years, has enabled making products with more industrial use potential than prototype products. In addition, AM has enabled the making of products of the same or better quality than traditional manufacturing methods for highly complex parts. The infill term, referring to the internal structure of an object printed in additive manufacturing, represents a stable structure selected by the user in the slicing software and a certain percentage of volume formed by this structure. The infill pattern and volume percentage significantly affect the printing process and the printed object's physical properties. Therefore, a high-volume percentage increases material consumption and printing time while producing parts that are more resistant to external loads [1]. In this context, experimental and theoretical studies have been conducted in the literature to determine the optimum infill geometries that can guide users in the design of light and mechanically robust prints [2,3]. For example, Deshpande et al. [4] investigated the effective mechanical properties of octet-lattice structures experimentally and theoretically. They stated that octet-lattice structures could be used as an alternative to metallic foams in porous structures. Baich et al. [5] investigated the interaction between filler designs and mechanical properties according to ASTM test standards and production cost time. They stated that continuous infill with the same production costs has higher strength under all loading conditions than double-layer intermittent filler. Vicente et al. [6] performed an experimental study to investigate the effect of filling patterns and density on the mechanical properties of acrylonitrile butadiene styrene (ABS) parts produced by AM. They stated that the difference in modulus of elasticity between honeycomb and linear patterns might be due to the different deposition trajectories and interlayer bonding regions between both patterns. Kumar et al. [7] stated in their studies that annealing and high filling density of FDM improved the mechanical properties of the samples printed with Polyethylene Terephthalate Glycol (PETG) and Carbon Fiber reinforced Polyethylene Terephthalate Glycol (CFPETG) material. Ganeshkumar et al. [8] experimentally and theoretically investigated the effects of gyroid, rhombic, circular, octahedron, and honeycomb fillers on the mechanical properties of 3D-printed Polylactic Acid (PLA) parts. They stated that the honeycomb infill pattern exhibited better mechanical properties than other infill structures. Lubombo and Huneault [9] analyzed the mechanical properties of PLA samples produced with FDM using three infill densities and five infill patterns by tensile and bending tests. The results showed that the hexagonal filler type performed best in balancing tension and bending mechanical properties. On the other hand, in addition to static tests, there are also studies examining the effect of filler geometry and density on mechanical properties in parts produced with AM under dynamic loads, albeit slightly. Tsouknidas et al. [10] investigated the effects of filling geometry and density on the energy absorption capacity of cylindrical parts produced with PLA and stated that the filling density has the most substantial effect on energy absorption, followed by layer height and filling pattern, respectively.

In this study, the effect of infill geometry and porosity on the mechanical behavior of the part was investigated experimentally in PLA-based plastic products produced using AM technology. It is understood from the literature that the tensile and compression behavior of parts produced with AM in different infill geometries is generally examined. In the presented study, the effect of the porosity ratio and the filling geometry on the part's mechanical properties was determined by impact tests in addition to the tensile and compression behavior. For this purpose, experimental samples with different pore ratios were modeled and produced in Octet, Gyroid, and Cross fill geometries, which are recommended for industrial use. The samples were

PRINT ISSN: 2149-4916 E-ISSN: 2149-9373 © 2022 Gazi Akademik Yayıncılık

modeled according to the relevant test standards and produced using a 3D printer based on the FDM method. Finally, it is aimed to contribute to the literature by determining the most suitable filling geometry and porosity ratio based on the considered mechanical properties.

2. Material and Methods

2.1. Material and Infill Geometry

In this study, three different infill geometries, Octet, Gyroid, and Cross, and three different porosity ratios (20%, 30%, and 50%) were decided apart from previous studies. Figure 1 shows the infill geometries selected for the test samples. Accordingly, parametric designs of Polylactic Acid (PLA) based samples were made for tensile, compression, and impact tests using 3D CURA software. The temperature was kept constant during the production of the samples. In the FDM-based additive manufacturing process, the most proper production parameters (such as printing speed, temperature, and construction direction) for the selected plastic material were obtained from the studies in the literature [11]. Some mechanical and physical properties of PLA used in the study are given in Table 1.

Table 1 Mechanical and physical properties of PLA [12]

Density	Melt Flow Rate	Melting Temperature	Tensile Strength	Impact Strength	Glass Transition Temperature, T_g
1.24 g/cc	7-9 g/10 dk.	165-180 °C	43 MPa	0.310 J	55-60 °C

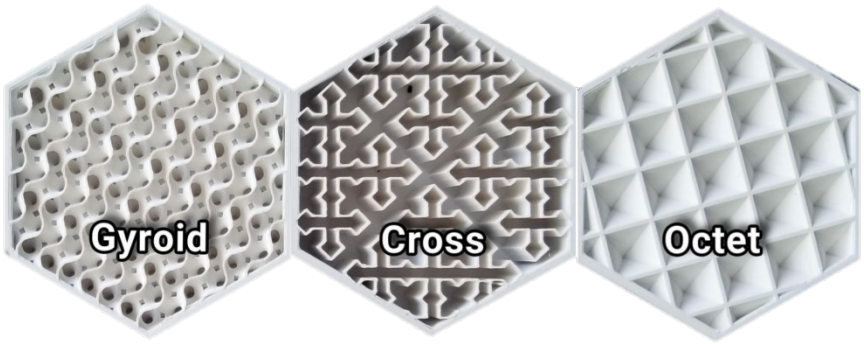

Figure 1 Unit cell structures used for infills [13].

2.2. Design and Production of Samples

Compression tests were carried out per the ASTM D695 standard, used in determining the rigid plastics' compression properties, to examine the effect of infill geometry and porosity ratio on the mechanical compression properties. To this end, Octet, Gyroid, and Cross unit cell shaped compression samples were designed with external dimensions of 25mm×25mm×25mm and pore ratios of 20%, 30%, and 50%. Additionally, relative density is an essential property used to characterize the mechanical behavior of cellular materials. Therefore, in the study, the porosity ratios of the samples were adjusted without changing the unit cell dimensions (5×5×5, in mm), only by changing the cell filling rates. The designed compression samples were produced using the FDM method from PLA material at a constant temperature (200 °C) in the Ultimaker additive manufacturing device [14].

For tensile strength of mechanical properties, samples with Octet, Gyroid, Cross unit cell structure, and 20-50% porosity ratios were designed and manufactured according to ASTM D638 standard. ASTM-D638 standard is a test method used to determine the tensile properties of rectangular plastic specimens. This standard has five different types of test specimens that can be used for reinforced composites, rigid, semi-rigid, non-rigid plastics, and rigid pipes. Type 1 specimen, whose dimensions are given in Figure 2, was used for the tensile test. The tensile specimens were produced using the 3D printer according to the above-mentioned manufacturing conditions.

PRINT ISSN: 2149-4916 E-ISSN: 2149-9373 © 2022 Gazi Akademik Yayıncılık

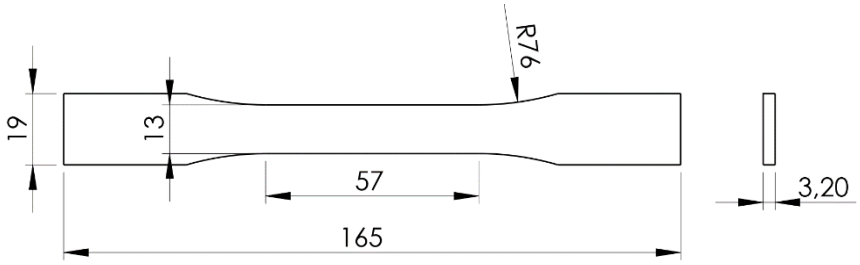

Figure 2. Type 1 specimen dimensions (mm)

Impact behavior was investigated as the third method in the analysis of the mechanical properties of PLA parts produced by additive manufacturing. For this purpose, unnotched 10x10x80 mm length samples with 20%, 30% and 50% filling ratios were produced in accordance with ISO 179 standard. The ISO 179 standard determines plastics' Charpy impact strength with pendulum-type testers. In design of these sample, octet, gyroid, and cross-unit cell shapes were used in the core of the structure. As with other mechanical property samples, the printing temperature for impact samples was set at 200°C.

3. Experimental Studies

To evaluate the effects of infill geometry and porosity ratio on the mechanical properties of the parts produced with FDM, tensile, compression, and impact tests were applied to the samples according to the relevant standards. In this context, compression tests were conducted according to the ASTM D1621 standard, which is used to determine the compressive behaviors of solid cellular plastics. An Instron tensile-compression test machine was used for the test. The loading speed was set at a constant 2 mm/min and carried out as a quasi-static compression test. The tests were carried out by turning each printed sample in the printing direction and perpendicular to the printing direction (90°). A total of 36 samples were tested by performing two retests for each sample. In addition, no lubricant was used on the contact surfaces between the sample and the plate during the experiments. The same test device was also used for the tensile test. Tensile tests were carried out per the ASTM D638 test standard, in the form of a semi-static tensile test, by applying a speed of 2 mm/min. The samples' tensile damage loads were determined using the force-elongation curves obtained at the end of the test. The examples of the images of the samples during and after the tensile test are given in Figure 3.

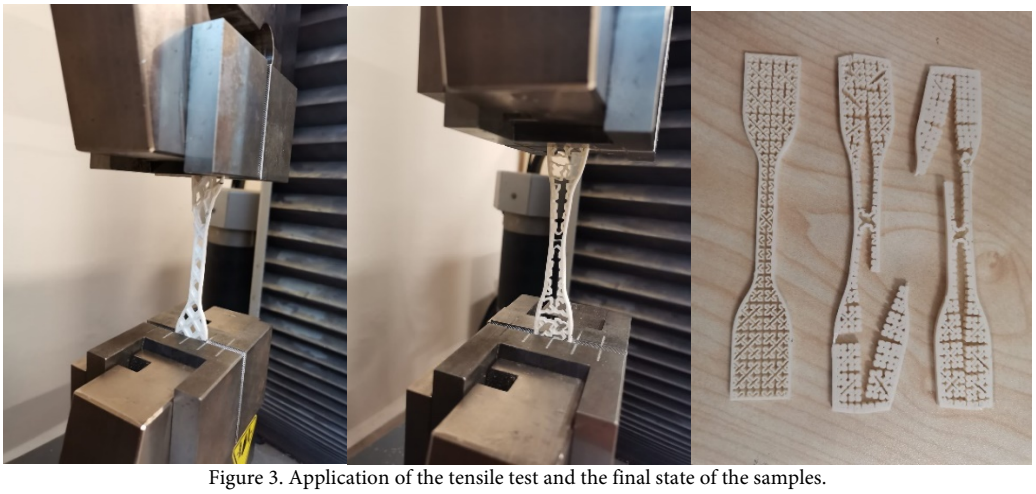

Figure 3. Application of the tensile test and the final state of the samples.

Impact tests were carried out according to the ISO 179 (Charpy test) standard to determine the impact resistance of the samples produced by the FDM method. Devotrans pendulum impact tester was used for Charpy impact tests. In the experiments, a hammer with a 152.7 g weight, suitable for the physical properties of the plastic material, was used. Samples were produced with the dimensions of 80x10x8 mm for the test. Additionally, shell structures with a thickness of 0.5 mm were formed on the samples' bottom, top and side surfaces. The steps of the impact test are shown in Figure 4.

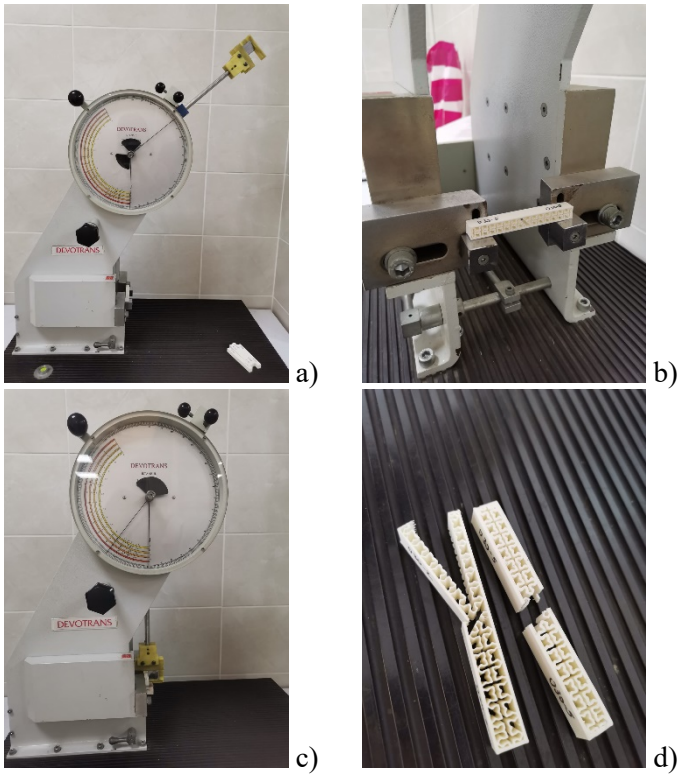

Figure 4. The stages of impact test: a) Initial position of the hammer on the test device, b) Sample binding, c) Impact location of the hammer on the test device, d) Sample view after the test [14].

4. Results and Discussions

4.1. Compression Test Results

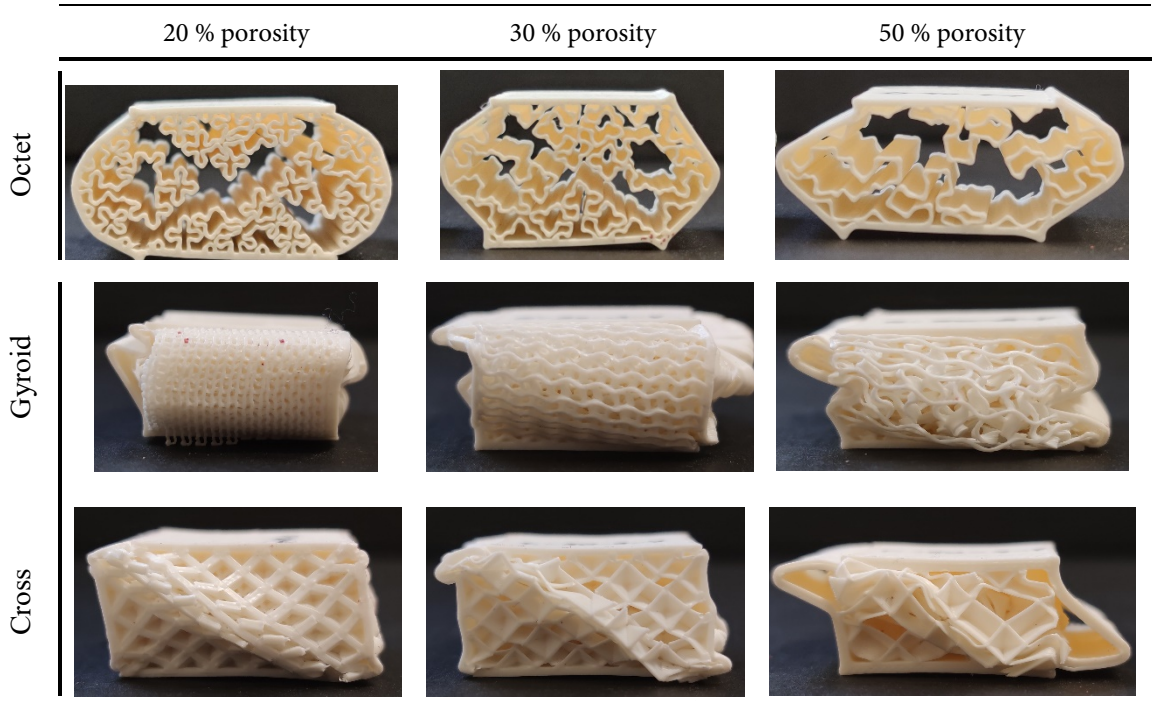

Figure 5. Shape changes in the samples at the end of the compression test.

To examine the effect of infill geometry (unit cell structure) and porosity ratio on the compressive strength

in PLA-based parts, six samples from each infill geometry were subjected to compression testing per ASTM D1621 standard. In Figure 5, the images of the samples after the compression test are given. In addition, the stress-strain diagrams obtained at the end of the compression test, depending on the change in the porosity ratio of the samples with Octet, Gyroid, and Cross unit cell structures, are given in Figure 6-8, respectively. The elastic modulus of the samples was calculated by considering the elastic region in the compressive stress-strain diagram and given in Table 1.

Table 1. Elasticity modulus and yield stress obtained by the compression test.

Modulus of Elasticity (MPa)						
	Perpendicular to the printing direction			**In printing direction**		
Porosity Ratio (%)	**Cross**	**Gyroid**	**Octet**	**Cross**	**Gyroid**	**Octet**
20	829.59	1107.50	135.42	874.40	926.77	1137.50
30	537.79	534.69	80.674	573.05	601.55	911.55
50	459.14	402.60	55.343	534.16	485.64	724.38
Yield Strength (MPa)						
20	15.72	18.43	1.180	18.01	16.16	18.75
30	9.29	9.21	0.708	10.71	9.83	13.08
50	8.18	5.58	0.646	9.87	7.05	9.86

In stress-strain diagrams obtained from compression tests of cellular structures and materials, it is stated that, generally, three deformation zones occur. These three regions are; the elastic region, called the pre-yielding stage, the plateau region formed after yielding, and the final compression region. The deformation behavior of these structures is classified as brittle or ductile depending on the plateau region's stress-strain values [15]. As can be seen from the graphs given in Figure 6-8, the stress-strain diagrams of the compression specimens consist of elastic, plateau, and final compression regions. Similar compression behaviors were obtained in different cellular structures [16]. When the compression behavior was evaluated in general, it was determined that the compressive elasticity modulus of the samples increased in all infill geometries with decreasing porosity. Structural anisotropy is one of the most critical parameters affecting the mechanical properties of porous parts produced with FDM. It has been stated that increasing the unit cell size of the cellular structure increases the printing sensitivity of the printer, which reduces the structural anisotropy of the additive manufacturing part [17]. Therefore, the structural anisotropy of the samples increased as the unit cell size of the fill geometry decreased. This formation caused an increase in the compressive elasticity modulus in samples with different fill geometry.

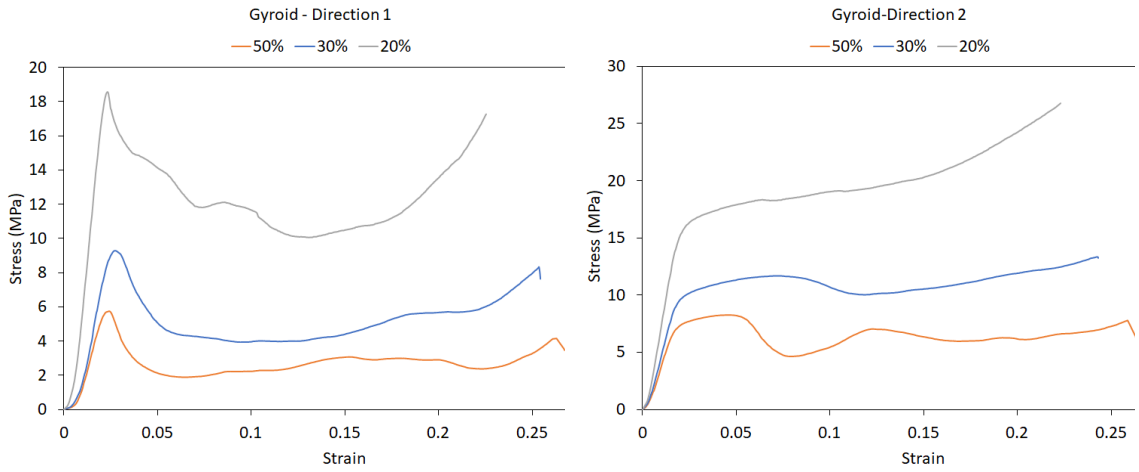

a) b)

Figure 6. Stress-strain diagrams of specimens with Gyroid infill geometry; a) Direction 1 (perpendicular to printing direction) b) Direction 2 (in printing direction).

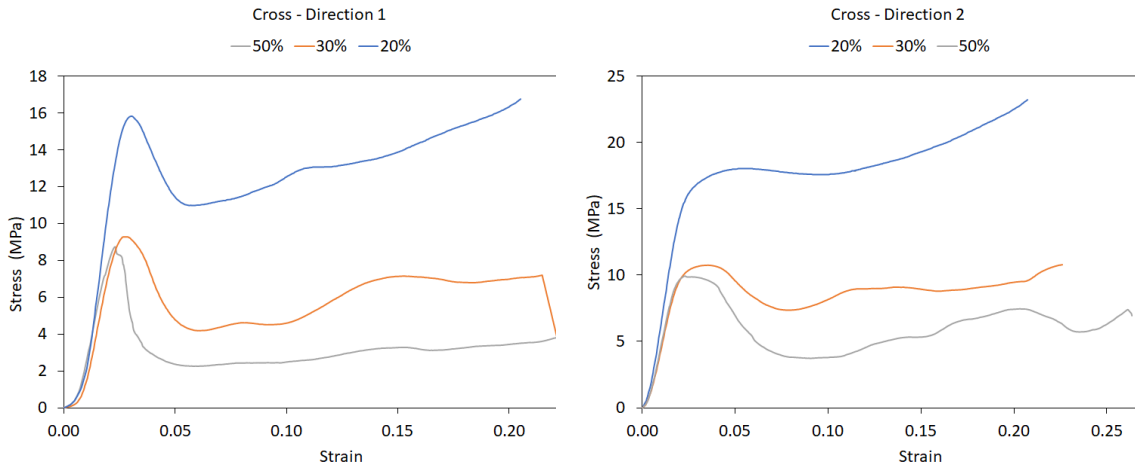

a) b)

Figure 7. Stress-strain diagrams of specimens with Cross infill geometry; a) Direction 1 (perpendicular to printing direction) b) Direction 2 (in printing direction).

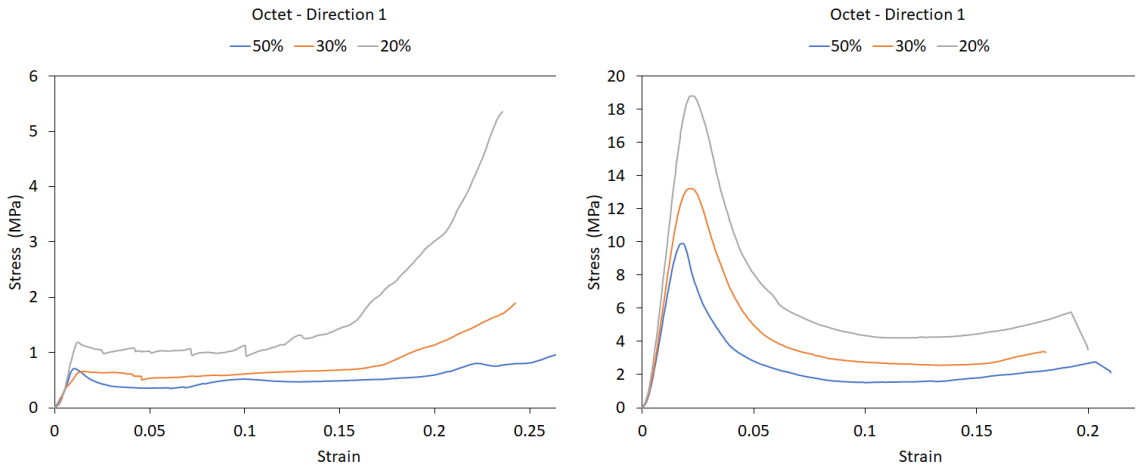

a) b)

Figure 8. Stress-strain diagrams of specimens with Octet infill geometry; a) Direction 1 (perpendicular to printing direction) b) Direction 2 (in printing direction).

The Octet infill geometry samples' elasticity modulus were obtained as 724.38 MPa, 911.55 MPa, and 1137.5 MPa on average for 50%, 30%, and 20% density ratios, respectively, by the compressing in the printing direction. However, these were obtained as 55.343 MPa, 80.674 MPa, and 135.42 MPa, respectively, by compressing perpendicular to the sample's printing direction. In the samples with gyroid infill geometry, the modulus of elasticity was obtained as 926.77 MPa, 601.55 MPa, and 485.64 MPa for the 50%, 30%, and 20% porosity ratios, respectively, by compressing the sample in the printing direction. In addition, compressive elasticity modules of 402.6 MPa, 534.69 MPa, and 1107.5 MPa were obtained for the specimen's compressed perpendicular to the printing direction. However, the compressive modulus of elasticities for specimens with Cross infill geometry were obtained as 534.16 MPa, 573.05 MPa, and 874.4 MPa in the printing direction for 50%, 30%, and 20% porosity ratios, respectively, and obtained as 459.14 MPa, 537.79 MPa and 829.59 MPa in the opposite to the printing direction. According to these results, the highest compressive elasticity modules and yield stresses were obtained in Octet infill geometry when the specimen was positioned vertically (in the printing direction). In contrast, the lowest compressive stress and elasticity modules were obtained when the specimen was positioned perpendicular to the printing direction. In addition, when the specimen was positioned horizontally (perpendicular to the printing direction), the highest compressive stresses and modulus of elasticity were obtained in the Cross infill geometry, except for the 20% porosity ratio. These

results show that the compression behavior of the parts may change according to the printing direction of the parts, according to the difference in the filling geometry as well as the material type [18].

4.2. Tensile Test Results

Three samples from each cell structure were subjected to tensile tests to determine the effect of infill geometry and porosity ratio on tensile strength. Samples prepared according to ASTM D638 standards were tested using an Instron tensile-compression tester. At the end of the test, the effects of the pore ratio and filler geometry on the tensile strength were examined by taking the average of the results obtained for the three samples.

The views of the samples after the tensile test are given in Figure 9. In the tensile tests of the filled samples produced by the FDM method, the fracture of the samples starts from the corners close to the sample holding jaws due to the stress concentrations caused by the diameter transitions. In the presented study, deformations occurred as fractures in the diameter transition region of the samples with Gyroid and Octet infill geometries. When the fracture patterns were examined, it was seen that some ductile deformation occurred due to the cellular structure. On the other hand, the deformation in Cross-infill geometry samples first occurred as the separation of the unit cells along the mid-symmetry line of the sample. Then it ruptured in the diameter transition region as in the Gyroid and Octet cell-filled samples.

a) Octet

b) Cross

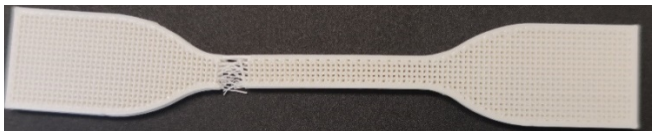

c) Gyroid

Figure 9. Views of the samples with a 20% porosity ratio after the tensile test.

The stress-strain diagrams of PLA samples with Octet, Gyroid, and Cross infill geometries depending on the change in porosity ratios are given in Figure 10, respectively. However, the sample's tensile modulus of elasticity was calculated by considering the elastic region in the stress-strain diagram. According to the infill geometry and porosity ratio, the modulus of elasticities were calculated as 37.70 MPa, 25.55 MPa, and 19.34 MPa in Cross infill samples, 34.13 MPa, 26.82 MPa, and 19.26 MPa in Gyroid infill samples, and 5.21 MPa, 4.87 MPa and 3.86 MPa in Octet infill samples, respectively, for 20%, 30%, and 50% porosity ratios. When the effect of the porosity ratio on the mechanical properties was evaluated, each sample's elasticity modulus decreased with increasing the porosity ratio from 20% to 50%. As mentioned in the literatures, these results showed that the tensile strength and modulus of elasticity decreased with decreasing density or increasing the pore ratio [19, 20], and indicated that the tensile behavior had a similar trend in different infill geometries. Besides, the elasticity modulus of Cross and Gyroid infill samples were higher than Octet infill samples at all porosity ratios.

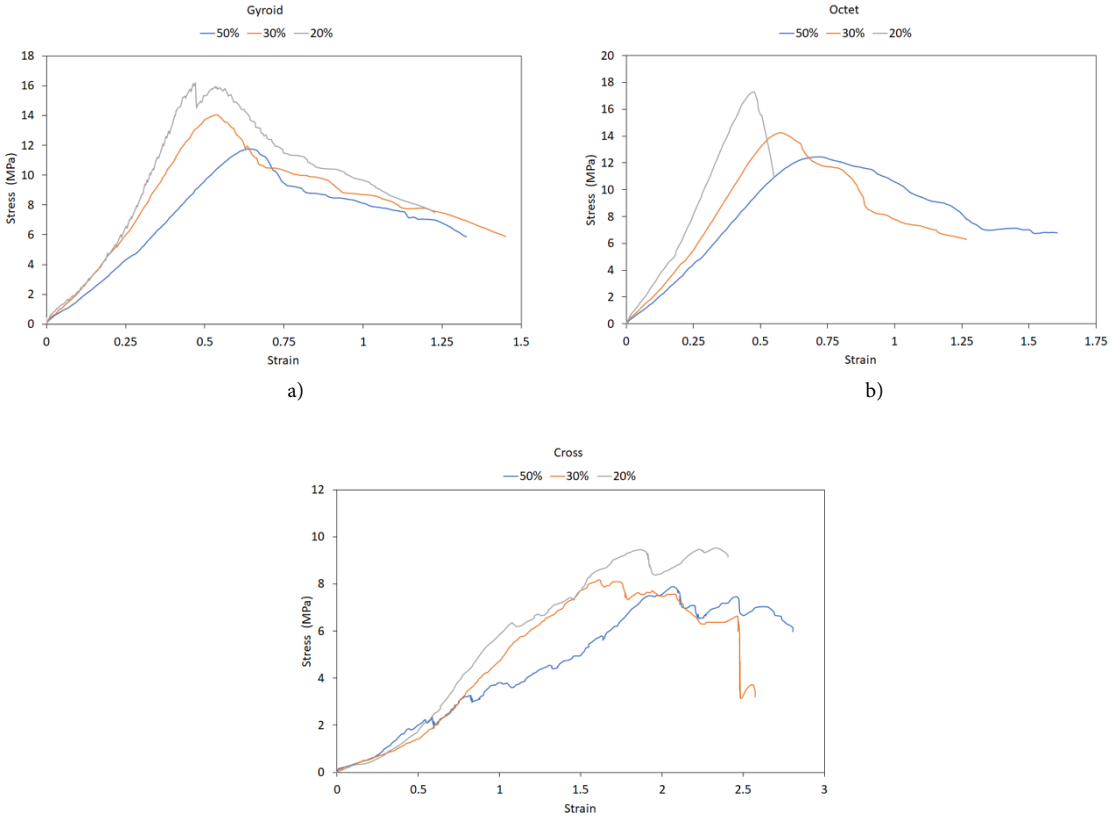

Figure 10. The effect of porosity ratio on tensile behavior of samples; a) Gyroid, b) Octet and c) Cross.

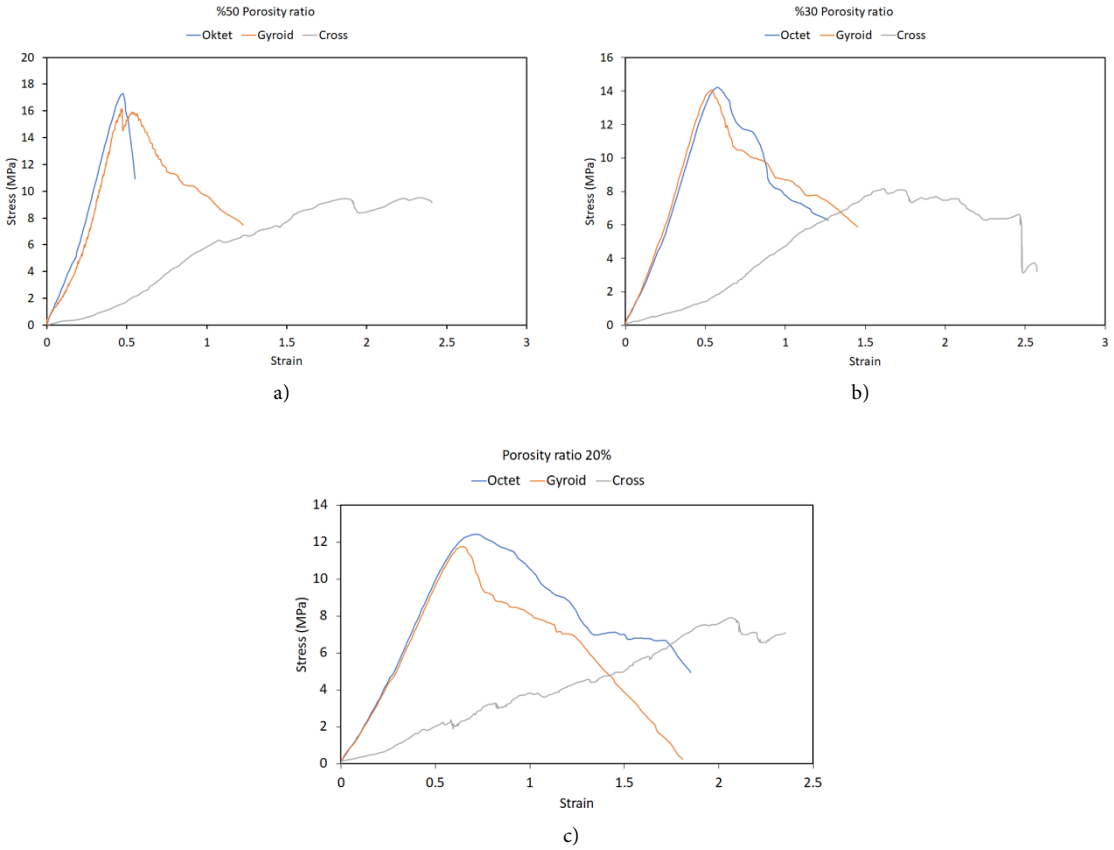

Figure 11. The effect of infill geometry on tensile behavior of samples; a) 50%, b) 30% and c) 20%.

Stress-strain diagrams in Figure 11 are given to evaluate the effect of infill geometry on tensile mechanical behavior of PLA specimens. When compared according to the infill geometry, it is seen that the Octet infill samples have the highest tensile strength in all porosity ratios. Slightly lower breaking stress values were obtained in the samples with Gyroid infill geometry compared to those with Octet infill geometry. However, while the lowest breaking stresses were obtained in Cross cell filled samples, higher deformations occurred compared to Octet and Gyroid infill samples.

4.3. Impact Test Results

The Charpy impact test was applied to the samples, prepared according to ISO 179 standard, to evaluate the effects of infill geometry and porosity ratio on the impact resistance in PLA-based parts. A 0.5 mm thick shell was formed on the sample's bottom, top, and side faces produced according to the standard, and the other two surfaces along the sample length were left open. The sample was positioned as Direction-1 and Direction-2 during the test according to the contact state of the hammer. In Direction-1 positioning, the sample is positioned so that its shell-covered face encounters the impact load of the hammer. However, in Direction-2 positioning, the sample is positioned so that its open face encounters the impact load of the hammer. The tests were carried out in two ways according to these directional positions. The appearances of the samples after the experiments are given in Figure 12.

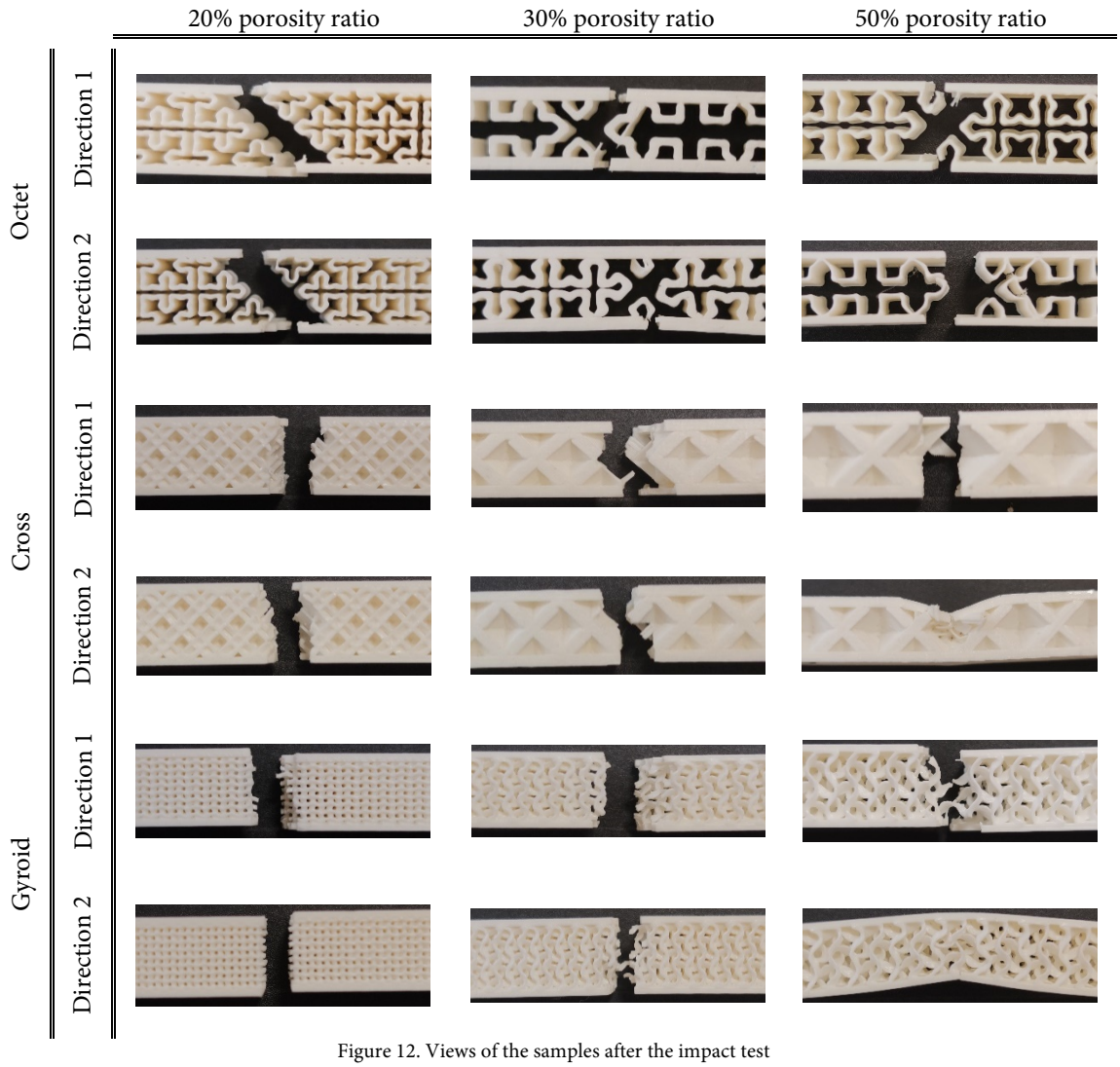

Figure 12. Views of the samples after the impact test

The impact resistances obtained when the samples are positioned as Direction-1 and Direction-2 are given in Figures 13a-13b, respectively. When the impact energies of the samples given in Figures 13a-13b are evaluated, the impact resistances of the Octet infill samples remain approximately the same. When the fracture pictures of the Octet samples obtained after the impact test were examined, the infill geometry could

not fulfill its task due to the insufficient connection between the infill patterns (Figure 12). This situation showed that the impact energy acting on the sample with Octet infill geometry was absorbed mainly by the sample's shell face. At the same time, it is seen that the breaks are not along a certain line. Thus, approximately the same impact energies were obtained. However, according to Figure 13, the impact resistances of the Gyroid infill samples increased as the pore ratio decreased. However, the impact resistances of Cross samples decreased by reducing the porosity ratio from 50% to 30% in Cross samples and then increased. In parallel with the literature [21], it was concluded that there is no linear relationship between the change in pore ratio and impact strength due to changing infill geometry.

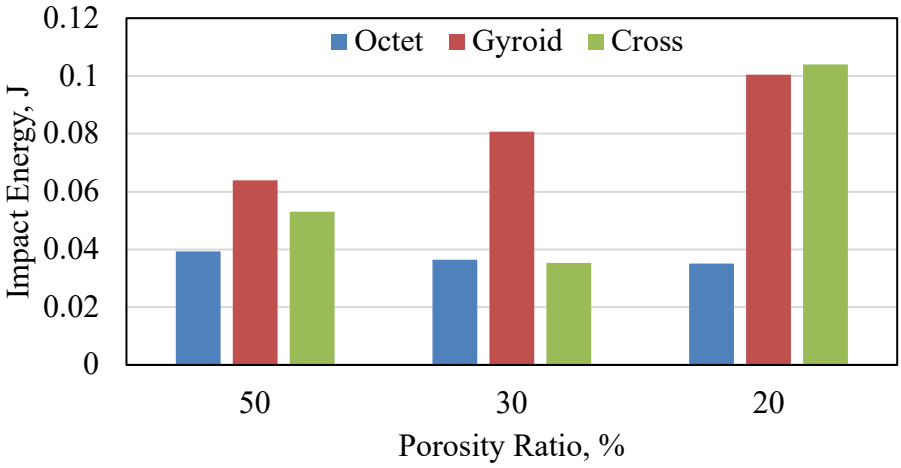

a)

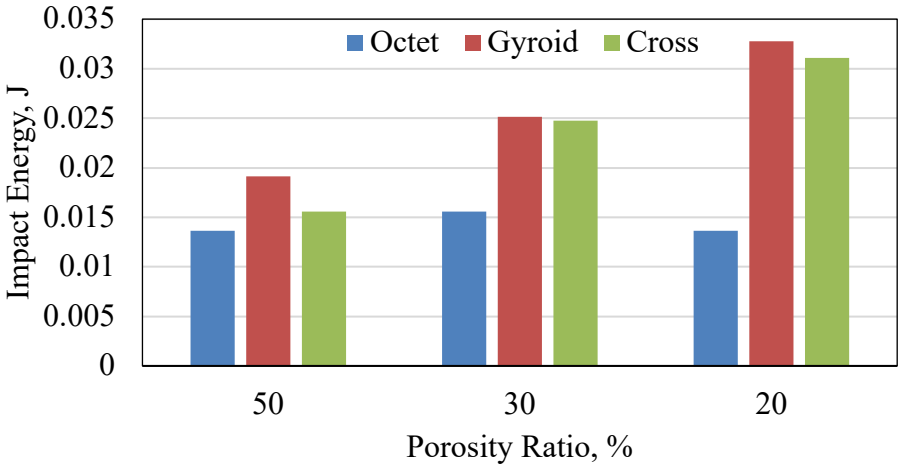

b)

Figure 13. Variation of impact energies with positioning samples for a) Direction 1, b) Direction-2

When the impact energies of the samples for Direction-2 are examined, it is seen that the impact resistances of the samples with Gyroid and Cross infill geometries decrease as the porosity ratio increases (Figure 13b). On the other hand, the impact resistances of the Octet infill samples remained approximately the same. However, it was determined that the impact resistances of Gyroid and Cross infill samples were higher than Octet infill samples at all porosity ratios. When a comparison is made in terms of the positioning of the samples as Direction-1 and Direction-2, it has been revealed that more impact energy can be absorbed in the Direction-2 positioning of the sample. In addition, it can be stated that the shell layer applied to the lower and upper surfaces of the samples increases the impact resistance. This result is attributed to the increasing density towards the sample surface as mentioned in the literature [22].

PRINT ISSN: 2149-4916 E-ISSN: 2149-9373 © 2022 Gazi Akademik Yayıncılık

5. Conclusions

In this study, the mechanical behavior of PLA-based parts produced with three different infill geometries (Gyroid, Cross, and Octet) and porosity ratios (20%, 30%, and 50%) by FDM additive manufacturing method was investigated by applying tensile, compression and impact tests. The main findings obtained from the experimental studies, carried out per the related standards, are summarized below:

- When the compressive behavior of the samples was evaluated, increasing the porosity ratio decreased the compressive elasticity modulus and yield stress of the samples. However, each infill geometry showed different responses to compression load at the same porosity ratio.
- The lowest compressive elasticity modulus and yield stress were obtained in Octet infill geometry when the samples were compressed horizontally (perpendicular to the construction direction). When the samples were compressed vertically (in the direction of construction), the lowest compressive elasticity modulus occurred in the Cross infill geometry and the lowest yield stress in the Gyroid infill geometry.
- When the tensile behavior is examined, increasing the porosity ratio increases the tensile modulus of elasticity. The highest tensile strength and modulus of elasticity were obtained in Octet infill geometry. However, the lowest tensile strength, modulus of elasticity, and highest deformations were obtained in the Cross infill geometry.
- When an evaluation is made in terms of impact resistance, the impact resistance increases as the porosity ratio decreases in the structure with Gyroid infill geometry. The lowest impact resistance was obtained in all porosity ratios in samples with Octet infill geometry. In addition, it was observed that the shell structure, added to the outside of the samples, increased their impact resistances.

Acknowledgment

The authors would like to thank Karabük University Coordinatorship of Scientific Research Projects for the financial support with project number FDT-2020-2062. This research is supported in part by Karabuk University.

Conflict of Interest Statement

The authors declare that there is no conflict of interest

References

[1] J. Wu, N. Aage, R. Westermann and O. Sigmund, "Infill Optimization for Additive Manufacturing-Approaching Bone-Like Porous Structures," *IEEE Trans. Vis. Comput. Graph.*, vol. 24, no. 2, pp. 1127-1140, January 2017. doi:10.1109/ TVCG.2017.2655523

[2] L. Lu, A. Sharf, H. Zhao, Y. Wei, Q. Fan, X. Chen, Y. Savoye, C. Tu, D. Cohen-Or and B. Chen, "Build-to-last: Strength to weight 3D printed objects," *ACM Trans. Graph.*, vol. 33, no. 4, pp. 1–10, July 2014. doi:10.1145/2601097.2601168

[3] W. Wang, T.Y. Wang, Z. Yang, L. Liu, X. Tong, W. Tong, J. Deng, F. Chen and X. Liu, "Cost-effective printing of 3D objects with skin-frame structures," *ACM Trans. Graph.*, vol. 32, no. 6, pp. 1-10, November 2013. doi:10.1145/ 2508363.2508382

[4] V.S. Deshpande, N.A. Fleck and M.F. Ashby, "Effective properties of the octet-truss lattice material," *J. Mech. Phys. Solids.*, vol. 49, no. 8, pp. 1747-1769, August 2001. doi:10.1016/S0022-5096(01)00010-2

[5] L. Baich, G. Manogharan and H. Marie, "Study of infill print design on production cost-time of 3D printed ABS parts," *Int. J. Rapid Manuf.*, vol. 5, no:3-4, pp 308-319, February 2016. doi:10.1504/ijrapidm.2015.074809

[6] M. Fernandez-Vicente, W. Calle, S. Ferrandiz and A. Conejero, "Effect of Infill Parameters on Tensile Mechanical Behavior in Desktop 3D Printing," *3D Print. Addit. Manuf.*, vol. 3, no. 3, pp. 183-1923, September 2016. doi:10.1089/3dp.2015.0036

[7] K.S. Kumar, R. Soundararajan, G. Shanthosh, P. Saravanakumar and M. Ratteesh, "Augmenting effect of infill density and annealing on mechanical properties of PETG and CFPETG composites fabricated by FDM," *Mater. Today Proc.*, vol. 45, no. 2, pp. 2186-2191, May 2021. doi:10.1016/j.matpr.2020.10.078

[8] S. Ganeshkumar, S.D. Kumar, U. Magarajan, S. Rajkumar, B. Arulmurugan, S. Sharma, C. Li, R.A. Ilyas and M.F. Badran, "Investigation of Tensile Properties of Different Infill Pattern Structures of 3D-Printed PLA Polymers: Analysis and Validation Using Finite Element Analysis in ANSYS," *Materials*, vol. 15, no. 15, pp. 5142, June 2022. doi:10.3390/ma15155142

[9] C. Lubombo and M.A. Huneault, "Effect of infill patterns on the mechanical performance of lightweight 3D-printed cellular PLA parts," *Mater. Today Commun.*, vol. 17, pp. 214-228, December 2018. doi:10.1016/j.mtcomm.2018.09.017

[10] A. Tsouknidas, M. Pantazopoulos, I. Katsoulis, D. Fasnakis, S. Maropoulos and N. Michailidis, "Impact absorption capacity of 3D-printed components fabricated by fused deposition modelling," *Mater. Des.*, vol. 102, pp. 41-44, July 2016. doi:10.1016/j.matdes.2016.03.154

[11] T. Yao, J. Ye, Z. Deng, K. Zhang, Y. Ma and H. Ouyang, "Tensile failure strength and separation angle of FDM 3D printing PLA material: Experimental and theoretical analyses," *Compos. Part B Eng.*, vol. 188, no. 107894, February 2020. doi:10.1016/j.compositesb.2020.107894

[12] "Essentium High Performance PLA Additive Manufacturing Filament," MatWeb, October 2022. [Online]. Available: https://www.matweb.com/index.aspx.

[13] "Infill Pattern Comparison". Reddit, June 2020. [Online]. Available: https://www.reddit.com/r/3Dprinting/comments/pdgbv0/infill_pattern_comparison/.

[14] R. Yeşiloğlu, "Eklemeli İmalat İle Üretilen Farklı Dolgu Geometrisi Ve Yoğunluğa Sahip Pla Esaslı Yapıların Mekanik Davranışlarının Deneysel Olarak Araştırılması," Y Lisans Tezi, Lisansüstü Eğitim Enstitüsü, Karabük Üniversitesi, 2022.

[15] Z. P. Sun, Y. B. Guo and V. P. W. Shim, "Deformation and energy absorption characteristics of additively-manufactured polymeric lattice structures - Effects of cell topology and material anisotropy," *Thin-Walled Struct.*, vol. 169, no. 108420, December 2021. doi:10.1016/j.tws.2021.108420

[16] A. Kumar, A. Kumar, A. Pandey, S. Sahu, N. Kumar and R. P. Singh, "Analysing the compressive behaviour of different PLA scaffolds fabricated through FFF process," *Advances in Materials and Processing Technologies*, vol. 9, no. 2, pp. 402-415, Jul 2022. doi:10.1080/2374068X.2022.2093005

[17] M. Alizadeh-Osgouei, Y. Li, A. Vahid, A. Ataee and C. Wen, "High strength porous PLA gyroid scaffolds manufactured via fused deposition modeling for tissue-engineering applications," *Smart Mater. Med.*, vol. 2, pp. 15-25, 2021. doi:10.1016/j.smaim.2020.10.003

[18] H. Dou, W. Ye, D. Zhang, Y. Cheng and Y. Tian, "Compression performance with different build orientation of fused filament fabrication polylactic acid, acrylonitrile butadiene styrene, and polyether ether ketone," *Journal of Materials Engineering and Performance*, vol. 31, pp. 1925–1933, 2022. doi:10.1007/s11665-021-06363-2

[19] M. Rismalia, S. C. Hidajat, I. G. R. Permana, B. Hadisujoto, M. Muslimin and F. Triawan, "Infill pattern and density effects on the tensile properties of 3D printed PLA material" *J. Phys.: Conf. Ser.*, vol. 1402, no. 4, 2019. doi:10.1088/1742-6596/1402/4/044041

[20] M. Günay, S. Gündüz, H. Yılmaz, N. Yaşar ve R. Kaçar, "PLA esasli numunelerde çekme dayanimi için 3D baski işlem parametrelerinin optimizasyonu," *Politeknik Dergisi*, cilt 23, sayı 1, ss. 73-79, 2020. doi:10.2339/ politeknik.422795

[21] S. Korga, M. Barszcz and Ł. Zgryza, "The effect of the 3D printout filling parameter on the impact strength of elements made with the FDM method," *IOP Conf. Series: Materials Science and Engineering*, vol. 710, 2019. doi:10.1088/1757-899X/710/1/012027

[22] M.Q. Tanveer, A. Haleem and M. Suhaib, "Effect of variable infill density on mechanical behaviour of 3-D printed PLA specimen: An experimental investigation." *SN Applied Sciences*, vol. 1, no. 1701, 2019. doi:10.1007/s42452-019-1744-1